

Research

CT-measured body composition radiomics predict lymph node metastasis in localized pancreatic ductal adenocarcinoma

Qianbiao Gu¹ · Mengqing He¹ · Yaqiong He¹ · Anqi Dai¹ · Jianbin Liu¹ · Xiang Chen¹ · Peng Liu¹

Received: 7 December 2022 / Accepted: 31 January 2023

Published online: 03 February 2023

© The Author(s) 2023 [OPEN](#)

Abstract

Background To explore the value of CT-measured body composition radiomics in preoperative evaluation of lymph node metastasis (LNM) in localized pancreatic ductal adenocarcinoma (LPDAC).

Methods We retrospectively collected patients with LPDAC who underwent surgical resection from January 2016 to June 2022. According to whether there was LNM after operation, the patients were divided into LNM group and non-LNM group in both male and female patients. The patient's body composition was measured by CT images at the level of the L3 vertebral body before surgery, and the radiomics features of adipose tissue and muscle were extracted. Multivariate logistic regression (forward LR) analyses were used to determine the predictors of LNM from male and female patient, respectively. Sexual dimorphism prediction signature using adipose tissue radiomics features, muscle tissue radiomics features and combined signature of both were developed and compared. The model performance is evaluated on discrimination and validated through a leave-one-out cross-validation method.

Results A total of 196 patients (mean age, 60 years \pm 9 [SD]; 117 men) were enrolled, including 59 LNM in male and 36 LNM in female. Both male and female CT-measured body composition radiomics signatures have a certain predictive power on LNM of LPDAC. Among them, the female adipose tissue signature showed the highest performance (area under the ROC curve (AUC), 0.895), and leave one out cross validation (LOOCV) indicated that the signature could accurately classify 83.5% of cases; The prediction efficiency of the signature can be further improved after adding the muscle radiomics features (AUC, 0.924, and the accuracy of the LOOCV was 87.3%); The abilities of male adipose tissue and muscle tissue radiomics signatures in predicting LNM of LPDAC was similar, AUC was 0.735 and 0.773, respectively, and the accuracy of LOOCV was 62.4% and 68.4%, respectively.

Conclusions CT-measured body composition Radiomics strategy showed good performance for predicting LNM in LPDAC, and has sexual dimorphism. It may provide a reference for individual treatment of LPDAC and related research about body composition in the future.

Keywords Body composition · Radiomics analysis · Computed tomography · Lymph node metastasis · Pancreatic ductal adenocarcinoma

Supplementary Information The online version contains supplementary material available at <https://doi.org/10.1007/s12672-023-00624-3>.

✉ Peng Liu, lpradiology@163.com; Qianbiao Gu, guqianbiao8@163.com | ¹Department of Radiology, Hunan Provincial People's Hospital, First Affiliated Hospital of Hunan Normal University, Changsha 410005, China.



Abbreviations

LNM	Lymph node metastasis
LPDAC	Localized pancreatic ductal adenocarcinoma
ROC	Receiver operating characteristic
AUC	Area under the curve
95%CI	95% Confidence interval

1 Introduction

Pancreatic cancer has a bleak prognosis, with a 5-year survival rate of less than 10% [1]. Based on the incidence of all malignant tumors, it ranks eighth among female patients and tenth among male patients. However, the total number of patients dying from pancreatic cancer is as high as third among all tumor-related causes of death, with the mortality rate increasing year by year [1, 2]. Surgical resection is the only cure for pancreatic cancer, with a 5-year survival rate of about 25% [3]. Accurate preoperative evaluation of lymph node status is the basis of personalized treatment of localized pancreatic ductal adenocarcinoma (LPDAC), which plays an important role in the treatment decision-making of patients. It has been reported that the 5-year survival rate of patients with lymph node metastasis (LNM) confirmed by postoperative pathology is similar to that of patients without surgical treatment, but that of patients without LNM is as high as 40% [4, 5]. Therefore, the prognosis of patients with different LN statuses varies greatly, who may require different extents of lymph node dissection or neoadjuvant therapy. NCCN guidelines recommend preoperative CT to evaluate the resectability of pancreatic cancer [6]. However, traditional CT imaging-based LNM evaluation methods have yielded disappointing results due to low sensitivity and specificity [7, 8]. Recently, radiomics has shown great potential in predicting LNM of pancreatic cancer [9–12]. However, these studies focus on the tumor itself, ignoring that pancreatic cancer is actually a systemic disease and a malignant tumor with metabolic heterogeneity. The change of amino acid, lipid metabolism and glucose in pancreatic cancer significantly affects tumor progression, from cell to microenvironment and even at the systemic level [13, 14].

Recently, tumor metabolic reprogramming has aroused great interest in researchers. Accumulating evidence supports the existence of dynamic changes in the metabolism of metastatic cells. A number of studies have found that fat-related metabolic changes are emerging factors in LNM [15–17], indicating an era of metabolic changes that make cancer cells into LNM. Computed tomography (CT) measured body composition, including subcutaneous and visceral fat and muscle, has been shown to be associated with systemic inflammatory immune and metabolic status. More importantly, it has been recognized as a predictor of many tumor and metabolic diseases [18–20].

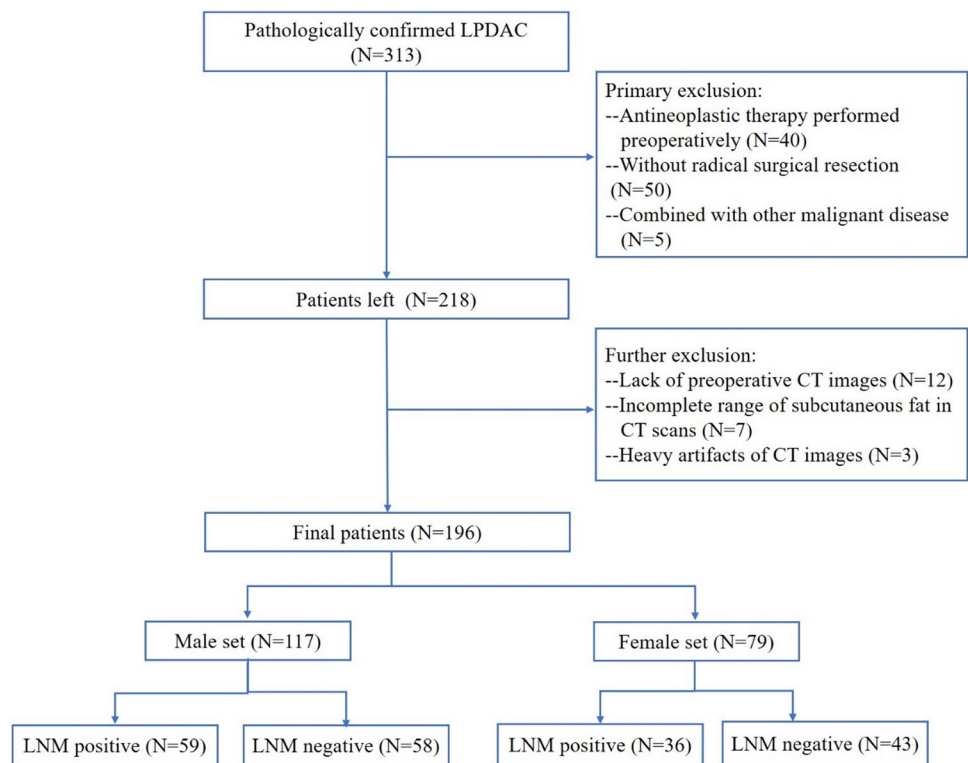
So far, no attempt has been made to predict the status of LNM in patients with pancreatic cancer based on human body composition radiomics. This study aims to explore whether CT-measured body composition radiomics can predict LNM in patients with LPDAC and whether there are gender differences in this method (Additional file 1).

2 Materials and methods

2.1 Patient data

This retrospective study received approval from the Institutional Review Board of our hospital, waiving the request for informed consent. Patients with LPDAC who accepted surgical resection in our hospital were retrospectively collected from January 2016 to June 2022. Inclusion criteria: 1. LPDAC was confirmed by postoperative pathology and immunohistochemistry examination. 2. A standard range of lymph node dissection was performed [21]. 3. CT scan was performed within 2 weeks before the operation. Exclusion criteria: 1. Antineoplastic therapy was performed preoperatively. 2. Patients with a history of other malignant diseases or concurrent primary cancers. 3. It is difficult to segment abdominal adipose tissue or skeletal muscle at the L3 level due to an incomplete scanning range of subcutaneous fat or excessive artifacts in CT images. The detailed process is shown in Fig. 1 This study included a total of 196 patients, including 79 females and 117 males.

Fig. 1 Patient flowchart for this study. *LPDAC* localized pancreatic ductal adenocarcinoma, *LNM* lymph node metastasis



2.2 Image acquisition

All patients accepted non-enhanced and enhanced CT scans of the upper abdomen or the whole abdomen (including arterial phase and venous phase) with Philips Brilliance iCT 256 or Siemens Somatom Force CT machine before the operation. The contrast agent iohexol 300 (300 mg/ml) was injected at a speed of 3 ml/s and a dose of 1.2–1.5 ml/kg through the anterior vein of the right elbow with an UlrichXD 2060 double-barrel high pressure syringe. Arterial phase and venous phase scans were conducted at 25–35 s and 60–70 s after injection, respectively, with scanning thickness of 2 mm, reconstruction thickness of 5 mm, automatic pitch matching, tube voltage of 120 kV, and tube current of 200–380 mA.

2.3 Body composition ROI segmentation

At present, most researchers have utilized the L3 vertebral body as the reference point for imaging-based body composition analysis [22, 23]. Therefore, body composition was measured by non-enhanced cross-sectional CT images at the L3 vertebral level to determine the region of adipose and muscle tissues. The adipose tissue included subcutaneous and visceral fat areas. Firstly, threshold-based ROI analysis was performed using the 3D Slicer software version 4.11.0 (www.slicer.org). Hounsfield unit (HU) thresholds were used as follows: adipose tissue from –190HU to –30HU; muscle tissue from –29HU to 150HU. Then, the mixed signals (such as intestinal content, caused by partial volume effect) were removed compared with the segmentation boundary of original CT images. It was segmented by two radiologists with 10 and 13 years of experience in abdominal imaging diagnosis, respectively.

2.4 Radiomics feature extraction

On the 3DSlicer platform, radiomics features were extracted from each patient's ROI using the open-source pyradiomic 3.0.1 version package. To obtain the isotropic voxels, ROI was resampled to 1 × 1 × 1 mm, and images were normalized to reduce the imaging differences between different CT scanning devices. To ensure better comparability

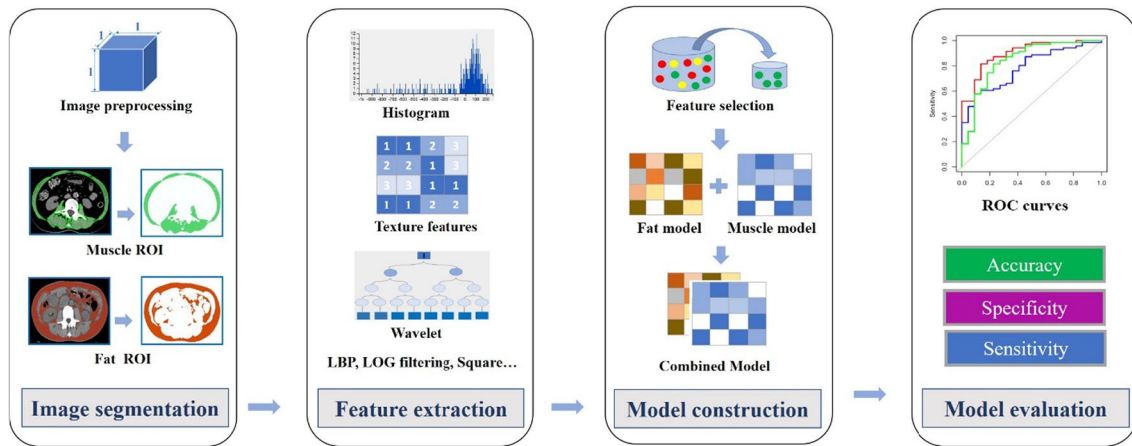


Fig. 2 Radiomics workflow and study flowchart. *ROI* region of interest, *ROC* Receiver Operating Characteristic

of CT gray values, a fixed slot width of 25 was chosen. Before feature extraction, the normalized CT image was filtered by gradient, index, logarithm, square root, wavelet, log filtering and other built-in filtering to obtain the derived image. Finally, 1,688 radiomics features were extracted from each ROI. The extracted features consisted of adjacent gray difference matrix (NGTDM), gray run matrix (GLRLM), gray size region matrix (GLSZM), gray dependence matrix (GLDM), gray co-occurrence matrix (GLCM), two-dimensional feature, and first-order feature [24]. Radiomics features are detailed in Additional file 1.

2.5 Radiomics feature selection and radiomics signature construction

The R software Caret package was used to pre-process the data. Firstly, zero variance and near-zero variance radiomics features were identified and removed with nearZeroVar in the caret package. Then, based on the Spearman test, radiomics features with a correlation coefficient greater than 0.9 and multiple collinearities were deleted, and independent features were preliminarily selected. Subsequently, to reduce the impact of dimensionality on the data and improve the comparability of different features, the data normalization procedure was performed, including mean-centred division by the standard deviation of each feature. Finally, multivariate logistic regression (forward LR) was used to screen for independent predictors of adipose and muscle in the LNM of pancreatic cancer among male and female patients. Moreover, sex-specific adipose and muscle radiomics signatures were established according to the selected radiomics features and the corresponding weight coefficients. (Fig. 2).

2.6 Statistical analysis

Statistical analysis was performed using IBM SPSS Statistics software (version 25) or R software (version 3.6.0; <http://www.r-project.org>). Continuous variables were represented as mean \pm SD, and categorical variables were compared using the χ^2 test. The area under the ROC curve (AUC), sensitivity and specificity were used to quantify the identification of the prediction signature. Leave one out cross validation was used to validate the prediction signature.

3 Results

3.1 Baseline characteristics

This study included a total of 196 patients, including 95 with LNM and 101 with non-LNM. Table 1 shows the basic clinical characteristics of these patients. No significant difference was found in sex, age, and longest tumor diameter

Table 1 Baseline characteristics of patients with pancreatic ductal adenocarcinoma

Characteristic	LNM (n=95)	Non-LNM (n=101)	P value
Sex			0.50
Male	59 (62)	58 (57)	
Female	36 (38)	43 (43)	
Age*	60 ± 10	60 ± 9	0.47
Longest diameter*	3.56 ± 1.63	3.52 ± 1.76	0.67
Location			0.03
Body or tail	16 (17)	36 (35)	
Head	79 (83)	65 (65)	

Except where indicated, data are numbers of patients, with percentages in parentheses

LNM lymph node metastasis

*Data are means ± SDs

between the LNM group and the non-LNM group ($P > 0.05$). There was a significant difference in the tumor location between the two groups ($P = 0.03$). It seemed that the tumor located in the pancreatic head was more prone to LNM.

3.2 Radiomics signature building

Among the 1688 radiomics features, 1211 features were retained after removing zero variance and near-zero variance radiomics features. Then, 329 independent radiomics features were selected through the correlation and collinearity tests. After splitting the cohort by gender, 5 radiomics features from adipose and 4 radiomics features from muscle were screened to predict LNM in male patients using the multivariate logistic regression (forward LR) method. The radiomics signature of male adipose with multivariate logistic regression was calculated using the following formula:

$$\begin{aligned}
 R_{\text{Smale}} - \text{fat} = & -3.790 * \text{gradient_firstorder_InterquartileRange} \\
 & + 0.682 * \text{gradient_glrlm_RunLengthNonUniformity} \\
 & + 0.658 * \text{gradient_glszm_SmallAreaLowGrayLevelEmphasis} \\
 & + 1.475 * \text{lbp.2D_firstorder_10Percentile} \\
 & + 0.655 * \text{wavelet.HHL_glcm_ClusterShade} - 0.453
 \end{aligned}$$

The radiomics signature of male muscle with multivariate logistic regression was calculated using the following formula:

$$\begin{aligned}
 R_{\text{Smale}} - \text{muscle} = & 1.035 * \text{wavelet.HHH_firstorder_Mean} \\
 & - 0.743 * \text{wavelet.HHH_firstorder_Skewness} \\
 & + 0.508 * \text{wavelet.HHH_gldm_LowGrayLevelEmphasis} \\
 & - 0.749 * \text{wavelet.HHH_glszm_SmallAreaEmphasis} + 0.287
 \end{aligned}$$

The sum of radiomics signature values of male muscle and adipose was used as a combined signature, namely:

$$R_{\text{Smale}} - \text{combined} = R_{\text{Smale}} - \text{fat} + R_{\text{Smale}} - \text{muscle}$$

Similarly, 7 radiomics features from adipose and 4 radiomics feature from muscle were screened to predict LNM in female patients using the multivariate logistic regression (forward LR) method. The radiomics signature of female adipose with multivariate logistic regression was calculated using the following formula:

Fig. 3 Performance of radiomics signature. *RS* radiomics score, *AUC* area under the curve

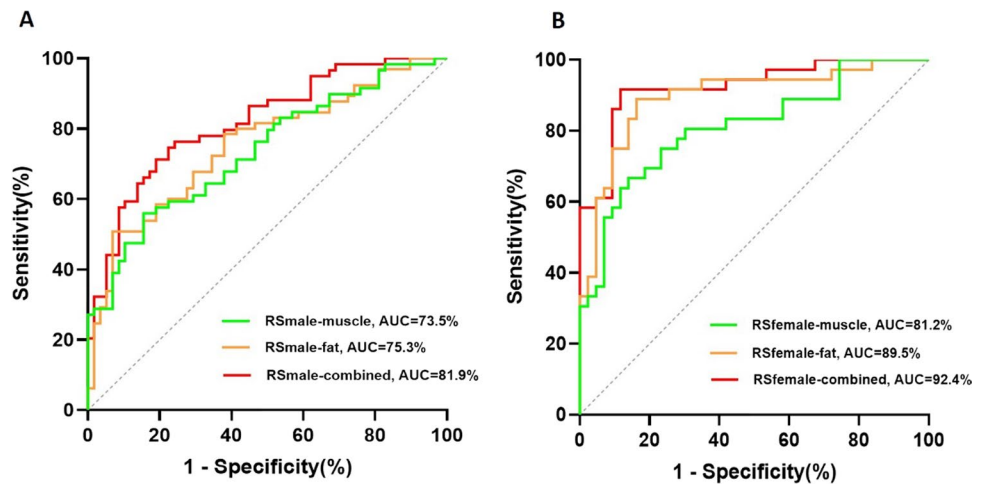


Table 2 Performance of Prediction Models for Predicting LNM of localized pancreatic ductal adenocarcinoma

Models	AUC (95% CI)	ACC	SEN	SPE	PPV	NPV
RS _{male-muscle}	0.735 (0.645, 0.825)	0.624	0.559	0.845	0.786	0.653
RS _{male-fat}	0.773 (0.689, 0.858)	0.684	0.525	0.931	0.886	0.659
RS _{male-combined}	0.819 (0.743, 0.894)	0.726	0.712	0.810	0.792	0.734
RS _{female-muscle}	0.811 (0.713, 0.908)	0.747	0.667	0.860	0.800	0.755
RS _{female-fat}	0.895 (0.821, 0.970)	0.835	0.889	0.837	0.821	0.900
RS _{female-combined}	0.924 (0.864, 0.984)	0.873	0.667	0.917	0.868	0.927

LNM lymph node metastasis, *RS* Radiomics signature, *AUC* area under the curve, *CI* confidence interval, *ACC* accuracy of leave one out cross-validation, *SEN* sensitivity, *SPE* specificity, *PPV* positive predictive value, *NPV* negative predictive value

$$\begin{aligned}
 RS_{female-fat} = & - 2.201 * \text{logarithm_glszm_LargeAreaHighGrayLevelEmphasis} \\
 & - 2.650 * \text{wavelet.HHL_glcm_Imc2} \\
 & + 1.749 * \text{wavelet.HHL_glszm_LowGrayLevelZoneEmphasis} \\
 & + 2.898 * \text{wavelet.HHL_glszm_ZoneEntropy} \\
 & - 3.256 * \text{wavelet.HLH_firstorder_Median} \\
 & + 1.630 * \text{wavelet.HLH_glszm_SmallAreaLowGrayLevelEmphasis} \\
 & - 2.064 * \text{wavelet.HLL_glcm_ldmn} - 1.384
 \end{aligned}$$

The radiomics signature of female muscle with multivariate logistic regression was calculated using the following formula:

$$\begin{aligned}
 RS_{female-muscle} = & 1.002 * \text{wavelet.HHH_firstorder_Minimum} \\
 & + 1.413 * \text{wavelet.HLH_glszm_GrayLevelVariance} \\
 & + 0.633 * \text{wavelet.LHH_glrlm_LongRunLowGrayLevelEmphasis} \\
 & - 0.996 * \text{wavelet.LHH_glszm_SmallAreaLowGrayLevelEmphasis} - 0.597
 \end{aligned}$$

The sum of radiomics signature values of female muscle and adipose was used as a combined signature, namely:

$$RS_{female-combined} = RS_{female-fat} + RS_{female-muscle}$$

3.3 Performance of radiomics signature

Both male and female CT-measured body composition radiomics signatures have a certain predictive power on LNM of LPDAC. For female patients, the AUC of adipose signature showed the highest performance at 0.895 (95% CI 0.821, 0.970), and leave one out cross validation (LOOCV) showed the signature could accurately classify 83.5% of cases. Moreover, the prediction efficiency of the signature can be further improved after adding the muscle radiomics features (AUC, 0.924 (95% CI 0.864, 0.984), and the accuracy of the LOOCV was 87.3%. For male patients, The prediction ability of adipose radiomics signature was similar to the radiomics signature of muscle, with an AUC of 0.735 (95% CI 0.645, 0.825), and 0.773 (95% CI 0.689, 0.858), respectively, and the accuracy of LOOCV was 62.4% and 68.4%, respectively. (Fig. 3). Table 2 shows the NPV, PPV, sensitivity, and accuracy of each model.

4 Discussion

Metabolic reprogramming is a sign of a malignant tumor, and tumor metastasis to lymph nodes requires abnormal metabolic transformation. The relationship between body composition that reflects host metabolism and lymph node metastasis of pancreatic cancer has not been reported. Hence, the purpose of this study is to design a gender-specific body composition radiomics method to predict LNM in patients with localized pancreatic cancer (LPDAC). Both adipose and muscle radiomics signature show good distinguishing ability for predicting LNM of LPDAC, and the female combined radiomics signature shows the best performance [AUC, 0.924].

According to the PDAC radiology reporting template proposed by the American Pancreatic Association and the Society of Abdominal Radiology, the diameter of regional LNs larger than 1 cm or other abnormal imaging signs are suspected to be involved [25]. However, this standard has performed poorly in many previous studies and our previous studies. All of these suggest that it is still very difficult for radiologists to predict lymph node metastasis.

At present, some studies have begun to use radiomics strategies to predict LNM in patients with pancreatic cancer. Li et al. reported a radiomics model with an AUC value of 0.91 in the validation set and 0.94 in the training set [9]. Liang et al. developed a radiomics nomogram with an AUC value of 0.80 in the primary cohort and 0.78 in the validation cohort [10]. Gao et al. established a radiomics model with good performance, which was similar to Liu et al. [11, 12]. Bian et al. directly focused on the lymph node itself, combined with artificial intelligence, and obtained the best performance (AUC, 0.92) [26]. However, these studies ignored the fact that pancreatic cancer is a systemic disease and the role of body composition changes in the prediction of LNM. Previous studies have shown that lymph nodes are considered a lipid-rich microenvironment, in which LNM tumor cells may give priority to the use of fatty acids as energy [15]. Rupert et al. reported that there is signal loop crosstalk between tumor-fat-muscle [27]. The deep-learning radiomics model established by An et al. showed that the model is most concerned with the tissue surrounding the tumor, rather than the tumor itself [28]. All of these suggest the value of body composition (adipose, muscle) in the assessment of LNM. Based on the above, this study focuses on body composition and uses a new quantitative radiomics strategy to explore the value of body composition-based radiomics in predicting the LNM of LPDAC.

This study was conducted on sexual dimorphism. As one of the earliest and most important advances in personalized medicine, sex-specific medicine has received great attention. It has been deeply studied in obesity, cancer, cardiovascular disease and other diseases [29]. There are significant differences in the distribution pattern and quality of adipose and muscle between sex [30–33]. This study found that Both male and female CT-measured body composition radiomics signatures have a certain predictive power on LNM of LPDAC. Among them, the female adipose signature showed the highest performance. Further analysis also showed that the predictive efficiency of body composition radiomics features in female patients was better than that in male patients. It is speculated that this may be related to the influence of sex-related hormones, and the underlying pathophysiological mechanism remains to be further investigated.

Although this study has tried to avoid the methodological issues of Radiomics in pancreatic tumors discussed by Bezzi C et al. [34], there are still several limitations in this study. First, the sample size of this study is small, especially for different gender groups. Second, a single slice of 2D features is used, rather than 3D features, based on the fact that the whole abdomen 3D segmentation of adipose and muscle or deep learning-based segmentation may be more representative of the body composition statue. Third, this study lacks an external validation of radiomics features. To obtain high-level evidence of clinical application, multicenter validation is required with larger sample size. Finally, clinical biochemical indicators such as Ca199 are not included as the purpose of this study is to focus on the predictive value

of body components for LNM, which preliminarily proves the feasibility of body composition radiomics based on CT images to predict LNM of LPDAC. To further improve the accuracy of preoperative assessment of the lymph node status of pancreatic cancer, further work is expected to combine tumors, lymph nodes, and body components to develop a multidimensional predictive model.

In summary, this study demonstrated the feasibility of CT-measured body composition radiomics in predicting LNM of pancreatic cancer, with sexual dimorphism differences. It may provide a reference for personalized diagnosis and treatment of pancreatic cancer and related research on body composition in the future.

Acknowledgements Not applicable.

Author contributions QG, PL, and YH participated in the design of the study. QG, MH, and PL wrote the manuscript. MH, AD, XC, JL, and QG collected and analyzed the data. PL, JL, MH, YH and QG contributed to interpretation of data and preparation of the manuscript. All authors read and approved the final manuscript.

Funding The China International Medical Foundation SKY Imaging Research Fund (No. Z-2014-07-2101); Scientific Research Project of Hunan Health Commission in 2022 (No. 202209010030); Clinical Medical Technology Innovation Guiding Project of Hunan Province (2021SK50911).

Data availability The datasets used and analysed during the current study are available from the corresponding author on reasonable request.

Declarations

Ethics approval and consent to participate This retrospective study received approval from the Hunan Provincial People's Hospital, First Affiliated Hospital of Hunan Normal University Review Board, waiving the request for informed consent. All the authors have followed the applicable ethical standards to maintain the research integrity without any duplication, fraud or plagiarism issues.

Consent for publication Not applicable.

Competing interests None.

Open Access This article is licensed under a Creative Commons Attribution 4.0 International License, which permits use, sharing, adaptation, distribution and reproduction in any medium or format, as long as you give appropriate credit to the original author(s) and the source, provide a link to the Creative Commons licence, and indicate if changes were made. The images or other third party material in this article are included in the article's Creative Commons licence, unless indicated otherwise in a credit line to the material. If material is not included in the article's Creative Commons licence and your intended use is not permitted by statutory regulation or exceeds the permitted use, you will need to obtain permission directly from the copyright holder. To view a copy of this licence, visit <http://creativecommons.org/licenses/by/4.0/>.

References

1. Siegel RL, Miller KD, Fuchs HE, Jemal A. Cancer statistics, 2022. *CA Cancer J Clin.* 2022;72(1):7–33.
2. Rawla P, Sunkara T, Gaduputi V. Epidemiology of pancreatic cancer: global trends, etiology and risk factors. *World J Oncol.* 2019;10(1):10–27.
3. Katz MH, Hwang R, Fleming JB, Evans DB. Tumor-node-metastasis staging of pancreatic adenocarcinoma. *J Clin.* 2008;58(2):111–25.
4. Lahat G, Lubezky N, Gerstenhaber F, Nizri E, Gysi M, Rozenek M, et al. Number of evaluated lymph nodes and positive lymph nodes, lymph node ratio, and log odds evaluation in early-stage pancreatic ductal adenocarcinoma: numerology or valid indicators of patient outcome? *World J Surg Oncol.* 2016;14(1):254.
5. Yamada M, Sugiura T, Okamura Y, Ito T, Yamamoto Y, Ashida R, et al. Clinical implication of node-negative resectable pancreatic cancer. *Ann Surg Oncol.* 2021;28(4):2257–64.
6. Network NCC. NCCN guidelines version 1. 2020. Pancreatic Adenocarcinoma. https://www.nccn.org/professionals/physician_gls/pdf/pancreatic.pdf.
7. Prenzel KL, Hölscher AH, Vallböhmer D, Drebber U, Gutschow CA, Mönig SP, et al. Lymph node size and metastatic infiltration in adenocarcinoma of the pancreatic head. *Eur J Surg Oncol.* 2010;36(10):993–6.
8. Imai H, Doi R, Kanazawa H, Kamo N, Koizumi M, Masui T, et al. Preoperative assessment of para-aortic lymph node metastasis in patients with pancreatic cancer. *Int J Clin Oncol.* 2010;15(3):294–300.
9. Li K, Yao Q, Xiao J, Li M, Yang J, Hou W, et al. Contrast-enhanced CT radiomics for predicting lymph node metastasis in pancreatic ductal adenocarcinoma: a pilot study. *Cancer Imaging.* 2020;20(1):12.
10. Liang X, Cai W, Liu X, Jin M, Ruan L, Yan S, et al. A radiomics model that predicts lymph node status in pancreatic cancer to guide clinical decision making: a retrospective study. *J Cancer.* 2021;12(20):6050–7.
11. Gao J, Han F, Jin Y, Wang X, Zhang J. A radiomics nomogram for the preoperative prediction of lymph node metastasis in pancreatic ductal adenocarcinoma. *Front Oncol.* 2020;10:1654.
12. Liu P, Gu Q, Hu X, Tan X, Liu J, Xie A, et al. Applying a radiomics-based strategy to preoperatively predict lymph node metastasis in the resectable pancreatic ductal adenocarcinoma. *J X Ray Sci Technol.* 2020;28(6):1113–21.
13. Qin C, Yang G, Yang J, Ren B, Wang H, Chen G, et al. Metabolism of pancreatic cancer: paving the way to better anticancer strategies. *Mol Cancer.* 2020;19(1):50.

14. Jeong DW, Lee S, Chun YS. How cancer cells remodel lipid metabolism: strategies targeting transcription factors. *Lipids Health Dis.* 2021;20(1):163.
15. Lee CK, Jeong SH, Jang C, Bae H, Kim YH, Park I, Kim SK, et al. Tumor metastasis to lymph nodes requires YAP-dependent metabolic adaptation. *Science.* 2019;363(6427):644–9.
16. Li M, Xian HC, Tang YJ, Liang XH, Tang YL. Fatty acid oxidation: driver of lymph node metastasis. *Cancer Cell Int.* 2021;21(1):339.
17. Zhu T, Wang Z, Zou T, Xu L, Zhang S, Chen Y, et al. SOAT1 promotes gastric cancer lymph node metastasis through lipid synthesis. *Front Pharmacol.* 2021;12:769647.
18. Aziz MH, van Dongen JC, Saida L, Suker M, van Vugt JLA, van Putten Y, et al. High systemic immune inflammation index is associated with low skeletal muscle quantity in resectable pancreatic ductal adenocarcinoma. *Front Oncol.* 2022;12:827755.
19. Pi-Sunyer X. Changes in body composition and metabolic disease risk. *Eur J Clin Nutr.* 2019;73(2):231–5.
20. Fehrenbach U, Wuensch T, Gabriel P, Segger L, Yamaguchi T, Auer TA, et al. CT body composition of sarcopenia and sarcopenic obesity: predictors of postoperative complications and survival in patients with locally advanced esophageal adenocarcinoma. *Cancers.* 2021;13(12):2921.
21. Tol JA, Gouma DJ, Bassi C, Dervenis C, Montorsi M, Adham M, et al. Definition of a standard lymphadenectomy in surgery for pancreatic ductal 236 adenocarcinoma: a consensus statement by the International Study Group on Pancreatic Surgery (ISGPS). *Surgery.* 2014;156(3):591–600.
22. Magudia K, Bridge CP, Bay CP, Babic A, Fintelmann FJ, Troschel FM, et al. Population-scale CT-based body composition analysis of a large outpatient population using deep learning to derive age-, sex-, and race-specific reference curves. *Radiology.* 2021;298(2):319–29.
23. Bridge CP, Best TD, Wrobel MM, Marquardt JP, Magudia K, Javidan C, et al. A fully automated deep learning pipeline for multi-vertebral level quantification and characterization of muscle and adipose tissue on chest CT scans. *Radiol Artif Intell.* 2022;4(1):e210080.
24. van Griethuysen JJM, Fedorov A, Parmar C, Hosny A, Aucoin N, Narayan V, et al. Computational radiomics system to decode the radiographic phenotype. *Cancer Res.* 2017;77(21):e104–107.
25. Al-Hawary MM, Francis IR, Chari ST, Fishman EK, Hough DM, Lu DS, et al. Pancreatic ductal adenocarcinoma radiology reporting template: consensus statement of the society of abdominal radiology and the american pancreatic association. *Gastroenterology.* 2014;146(1):291–304.
26. Bian Y, Zheng Z, Fang X, Jiang H, Zhu M, Yu J, et al. Artificial intelligence to predict lymph node metastasis at CT in pancreatic ductal adenocarcinoma. *Radiology.* 2022. <https://doi.org/10.1148/radiol.220329>.
27. Rupert JE, Narasimhan A, Jengelly DHA, Jiang Y, Liu J, Au E, et al. Tumor-derived IL-6 and trans-signaling among tumor, fat, and muscle mediate pancreatic cancer cachexia. *J Exp Med.* 2021. <https://doi.org/10.1084/jem.20190450>.
28. An C, Li D, Li S, Li W, Tong T, Liu L, et al. Deep learning radiomics of dual-energy computed tomography for predicting lymph node metastases of pancreatic ductal adenocarcinoma. *Eur J Nucl Med Mol Imaging.* 2022;49(4):1187–99.
29. Gemmati D, Varani K, Bramanti B, Piva R, Bonaccorsi G, Trentini A, et al. “Bridging the gap” everything that could have been avoided if we had applied gender medicine, pharmacogenetics and personalized medicine in the gender-omics and sex-omics era. *Int J Mol Sci.* 2019;21(1):296.
30. Liedtke S, Schmidt ME, Vrieling A, Lukanova A, Becker S, Kaaks R, et al. Postmenopausal sex hormones in relation to body fat distribution. *Obesity.* 2012;20(5):1088–95.
31. Oh C, Jho S, No JK, Kim HS. Body composition changes were related to nutrient intakes in elderly men but elderly women had a higher prevalence of sarcopenic obesity in a population of Korean adults. *Nutr Res.* 2015;35(1):1–6.
32. Du Y, Wang X, Xie H, Zheng S, Wu X, Zhu X, et al. Sex differences in the prevalence and adverse outcomes of sarcopenia and sarcopenic obesity in community dwelling elderly in East China using the AWGS criteria. *BMC Endocr Disord.* 2019;19(1):109.
33. Frank AP, de Souza SR, Palmer BF, Clegg DJ. Determinants of body fat distribution in humans may provide insight about obesity-related health risks. *J Lipid Res.* 2019;60(10):1710–9.
34. Bezzi C, Mapelli P, Presotto L, Neri I, Scifo P, Savi A, et al. Radiomics in pancreatic neuroendocrine tumors: methodological issues and clinical significance. *Eur J Nucl Med Mol Imaging.* 2021;48(12):4002–15.

Publisher's Note Springer Nature remains neutral with regard to jurisdictional claims in published maps and institutional affiliations.